

# Fast Rydberg gates without dipole blockade via quantum control

M. Cozzini<sup>a</sup>, T. Calarco<sup>a,b</sup>, A. Recati<sup>a</sup>, P. Zoller<sup>c</sup>

<sup>a</sup>*Dip. di Fisica, Università di Trento and BEC-CNR-INFN, I-38050 Povo, Italy*

<sup>b</sup>*ITAMP, Harvard-Smithsonian Center for Astrophysics, Cambridge,  
MA 02138, USA*

<sup>c</sup>*Institute for Quantum Optics and Quantum Information of the Austrian  
Academy of Sciences and Institut für Theoretische Physik, Universität Innsbruck,  
A-6020 Innsbruck, Austria*

---

## Abstract

We propose a scheme for controlling interactions between Rydberg-excited neutral atoms in order to perform a fast high-fidelity quantum gate. Unlike dipole-blockade mechanisms already found in the literature, we drive resonantly the atoms with a state-dependent excitation to Rydberg levels, and we exploit the resulting dipole-dipole interaction to induce a controlled atomic motion in the trap, in a similar way as discussed in recent ion-trap quantum computing proposals. This leads atoms to gain the required gate phase, which turns out to be a combination of a dynamic and a geometrical contribution. The fidelity of this scheme is studied including small anharmonicity and temperature effects, with promising results for reasonably achievable experimental parameters.

*Key words:* Quantum phase gate, Rydberg states

*PACS:* 03.67.Lx, 32.80.Pj, 32.80.Rm

---

## 1 Introduction

The quest for the reliable implementation of a fundamental quantum gate is one of the central topics in the current research in quantum computation. The basic requirement is the controlled coherent dynamics [1] of the system realizing the quantum bits, while avoiding decoherence due to fluctuations of the external control parameters and coupling to an environment<sup>1</sup>.

---

<sup>1</sup> We dedicate this publication to Bruce Shore as one of the pioneers in developing the theory of coherent interactions between atoms and laser light.

In the last years, several proposals for different physical systems have appeared, ranging from trapped ions [2], photons in cavity QED [3], molecules [4], to quantum dots and Josephson Junctions [5]. A particularly attractive perspective is the possibility of using cold neutral atoms [6], whose steadily improving experimental control looks quite promising. Regarding the required logical operations, different possible universal sets of quantum gates have been devised, showing that single-qubit and two-qubit gates are sufficient to realize any  $N$ -qubit unitary operator. In this context, a widely studied fundamental gate is the two-qubit controlled-phase gate, whose truth table is given by

$$\begin{aligned}
|g\rangle|g\rangle &\rightarrow e^{i\phi}|g\rangle|g\rangle \\
|g\rangle|e\rangle &\rightarrow |g\rangle|e\rangle \\
|e\rangle|g\rangle &\rightarrow |e\rangle|g\rangle \\
|e\rangle|e\rangle &\rightarrow |e\rangle|e\rangle ,
\end{aligned} \tag{1}$$

where  $\phi$  is the phase and  $|g\rangle$ ,  $|e\rangle$  are the logical states. When  $\phi$  equals  $\pi$ , this gate is equivalent to a Controlled-NOT and is universal if combined with arbitrary single-qubit rotations.

An important figure of merit to evaluate a specific physical implementation is the ratio between the gate operation time and the coherence time characteristic of the system. In this sense, for a given quantum memory coherence time and gate error rate, faster gates are of course highly preferable. However, gate speed is limited by several system-specific factors, for instance by the characteristic energy scales that are present: roughly speaking, if the phase  $\phi$  in Eq. (1) is produced by a state-dependent energy shift  $\Delta E$ , the time it takes for a phase  $\pi$  to be accumulated has to be of the order of  $\Delta E^{-1}$ .

In trapped atomic systems the relevant energy scales are the frequency of the trapping itself (which can hardly exceed, say, a few hundred kHz) and the energy of atom-atom interactions. This has led to several theoretical explorations towards employing stronger interactions like dipole-dipole forces between Rydberg-excited atoms [7] or molecular interactions giving rise to Feshbach resonances [8]. The main issue to be dealt with in this case is that strong interactions tend to perturb significantly the trapped-atom dynamics, thereby representing a potential source of errors. Ways around this problem depend again on the specific feature of the system under consideration. For instance, putting Rydberg atoms in a sufficiently stable and intense static electric field, a dipole-blockade mechanism can arise that shifts the two-atom interacting state out of resonance from single-atom exciting lasers [9,10]. In this case, a two-qubit gate can be performed without ever switching on the dipole-dipole interaction, thereby avoiding decoherence due to entanglement of the qubit with the motion.

An alternative way to overcome trap-limited gate time scales is to employ quantum control techniques, as originally proposed in the context of ion-trap quantum gates in [11]. In this approach, the gate phase is not directly or indirectly obtained from a state-selective energy shift due to interaction, but rather by driving the two-particle system on a closed path in phase space, whose final result is to bring it back to its original state, while at the same time imprinting on it the desired phase.

The present paper represents an application of these methods, developed in [11,12] for trapped ions, to the case of Rydberg-excited atoms already discussed in [7]. The use of quantum control techniques allows for exploiting the strong perturbation due to dipole-dipole interaction as a means for driving the system into the goal state with a high fidelity that does not depend, to a good approximation, on the initial motional state of both atoms inside the trap, and in a time that is a fraction of the trap period. Moreover, since the phase is not accumulated as a result of some interaction-induced energy shift as discussed above, the atoms are not required to remain in the interacting state for the whole duration of the gate, but just during much shorter times as needed for imparting the “kicks” which drive their motion. In this way the effect of decoherence due to spontaneous emission from the highly excited Rydberg states is further reduced.

A generic quantum computation requires in principle the ability to perform more complex sequences of two-qubit gates between any pair of qubits. To achieve this, one will need to move atoms between different locations in the quantum register. Thus the overall speed of a complete quantum computation in general will be basically limited by the time needed to transport the atoms close to one another before performing each actual gate operation on the desired qubit pairs. This limitation affects all quantum computing implementations based on atomic (or ionic) systems. However, it can be partially overcome by applying quantum control techniques to the transport process [13]. In addition, individual addressing, which is still an issue in present experiments, is not needed at the level of a two-qubit gate within the protocol proposed here, and therefore atoms can be kept during the gate at a shorter distance than required in other schemes by single-atom laser diffraction-limited addressability. Thus atom transport would only be required for two-qubit gates involving non-neighboring qubits, and it may be employed as well whenever a gate on a single qubit is needed during the computation, to single it out by moving it away from the other qubits.

The structure of the paper is as follows. In Sec. II we introduce in general terms the simple control procedure we plan to apply to the system for this purpose; in Sec. III we describe the physical model for the implementation of the control pulses with dipole-interacting atomic systems and discuss experimental parameters; and in Sec. IV we analyze quantitatively the obtainable

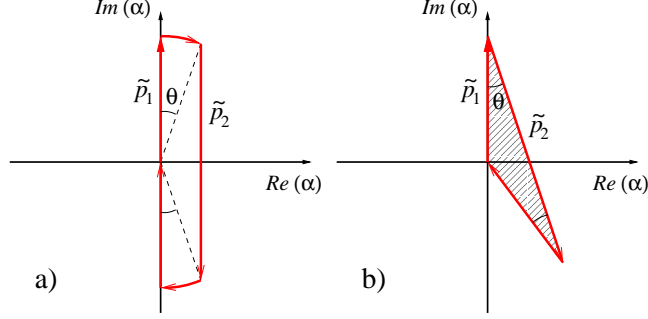


Fig. 1. Phase space trajectory of a simple kick protocol: a) usual reference frame; b) rotating reference frame. The harmonic oscillator ground state is first given a positive momentum  $p_1 = \sqrt{2}\tilde{p}_1$ ; then it is left evolve in the pure harmonic oscillator potential for a time  $\theta$  (in harmonic oscillator units), and hence kicked again by a negative momentum  $p_2 = \sqrt{2}\tilde{p}_2 = -2p_1 \cos(\theta)$ . The purely harmonic evolution time  $\theta$  corresponds to the angle shown in the figure. The final kick, which brings the system back to the initial coherent state, has the same intensity  $p_1$  as the first one.

fidelity, before drawing our conclusions in Sec. V.

## 2 Control scheme

We begin by discussing a possible ‘kick’ scheme to manipulate the system phase while bringing the atoms back to the initial motional state, in the spirit of Ref. [11]. Although in the next sections we will adapt this protocol to our particular configuration, we point out that this scheme is applicable to quite general systems. In this section, the ‘system’ is simply given by a single particle in a one-dimensional harmonic potential, corresponding in the following to the relative motion of the two atoms.

The basic idea is to lead the system along a closed path in the oscillator phase space by taking advantage of the momentum shifts – the so-called kicks – induced by some external force. The simplest possible protocol, i.e., that requiring the minimal number of kicks, is illustrated in Fig. 1 for the special case of the oscillator ground state. This scheme, as far as the kicks are ideal shifts (see the impulse approximation discussed in the next section), has the remarkable advantage of being independent of the initial state.

We consider the unitary phase space displacement operator  $D(\alpha) = e^{\alpha\hat{a}^\dagger - \alpha^*\hat{a}}$ , where  $\hat{a}^\dagger$  and  $\hat{a}$  are respectively the creation and annihilation operators of the harmonic oscillator and dimensionless units are used<sup>2</sup>. With this formalism, a kick of momentum  $p$  is simply given by  $e^{ip\hat{x}} = D(i\tilde{p})$ , where  $\tilde{p} = p/\sqrt{2}$  is a

<sup>2</sup> We recall that  $D(\alpha)|0\rangle = |\alpha\rangle$ , where  $|0\rangle$  is the oscillator ground state and the coherent state  $|\alpha\rangle$  is an eigenstate of the annihilation operator  $\hat{a}|\alpha\rangle = \alpha|\alpha\rangle$ .

real number and  $\hat{x} = (\hat{a} + \hat{a}^\dagger)/\sqrt{2}$  is the position operator. The protocol shown in Fig. 1 is a sequence of three kicks alternated by free harmonic evolution, the latter being governed by the harmonic time evolution operator  $U_{\text{ho}}(t) = e^{-i(\hat{a}^\dagger\hat{a} + 1/2)t}$ . By using the well known relations  $D(\alpha)D(\beta) = D(\alpha + \beta)e^{i\text{Im}(\alpha\beta^*)}$  and  $U_{\text{ho}}(t)D(\alpha) = D(e^{-it}\alpha)U_{\text{ho}}(t)$ , one can easily rewrite the kick operator  $G = D(i\tilde{p}_3)U_{\text{ho}}(\theta_2)D(-i\tilde{p}_2)U_{\text{ho}}(\theta_1)D(i\tilde{p}_1)$  in the form

$$G = U_{\text{ho}}(\theta_1 + \theta_2)D(i[\tilde{p}_1 - \tilde{p}_2e^{i\theta_1} + \tilde{p}_3e^{i(\theta_1+\theta_2)}])e^{i\phi_{\text{geom}}} , \quad (2)$$

where  $\phi_{\text{geom}} = \tilde{p}_1\tilde{p}_3 \sin(\theta_1 + \theta_2) - \tilde{p}_1\tilde{p}_2 \sin \theta_1 - \tilde{p}_2\tilde{p}_3 \sin \theta_2$ . The ‘triangle’ scheme is nothing but the condition  $\tilde{p}_1 - \tilde{p}_2e^{i\theta_1} + \tilde{p}_3e^{i(\theta_1+\theta_2)} = 0$ , so that  $G = U_{\text{ho}}(\theta_1 + \theta_2)e^{i\phi_{\text{geom}}}$  and the initial motional state is restored. The triangular path is evident in the rotating frame description (see Fig. 1(b)), namely the interaction picture where the action of the oscillator Hamiltonian  $H_{\text{ho}} = \hat{a}^\dagger\hat{a} + 1/2$  is made implicit and the gate operator does not contain the term  $U_{\text{ho}}(\theta_1 + \theta_2)$ . In addition, one immediately finds  $\tilde{p}_1\tilde{p}_2 \sin \theta_1 = \tilde{p}_2\tilde{p}_3 \sin \theta_2 = \tilde{p}_1\tilde{p}_3 \sin(\theta_1 + \theta_2) = 2A$ , where  $A$  is the area of the triangle described by the rotating phase space trajectory. Finally,  $\phi_{\text{geom}} = -2A$  and, for the considered case  $0 \leq \theta_1 = \theta_2 = \theta \leq \pi/2$ ,  $\phi_{\text{geom}} = -\tilde{p}_1^2 \sin(2\theta)$ . Being based on operatorial identities this result is evidently independent of the initial state. It is worth recalling the ‘geometric’ nature of such phase, as discussed in Ref. [12], reflected by the non-commutativity of the phase-space displacement operators.

We stress that the discussion in this section simply refers to the dynamics of a 1D harmonic oscillator. Below we will see that such scheme can be applied to the effective 1D oscillator obtained for the relative motion of the two considered atoms, so that this geometric phase will be used in a protocol for a two-qubit gate. The concrete implementation will however introduce some approximations whose validity will actually depend on the initial oscillator state (see Subsec. 3.3).

### 3 Physical implementation

We now turn to the analysis of the particular case where the kicks are provided by the switching of the dipole-dipole interaction. We will first give an overview of the actual form of the interaction, then we will discuss its application to the protocol presented in the previous section, and finally we will examine the validity conditions for the approximations introduced.

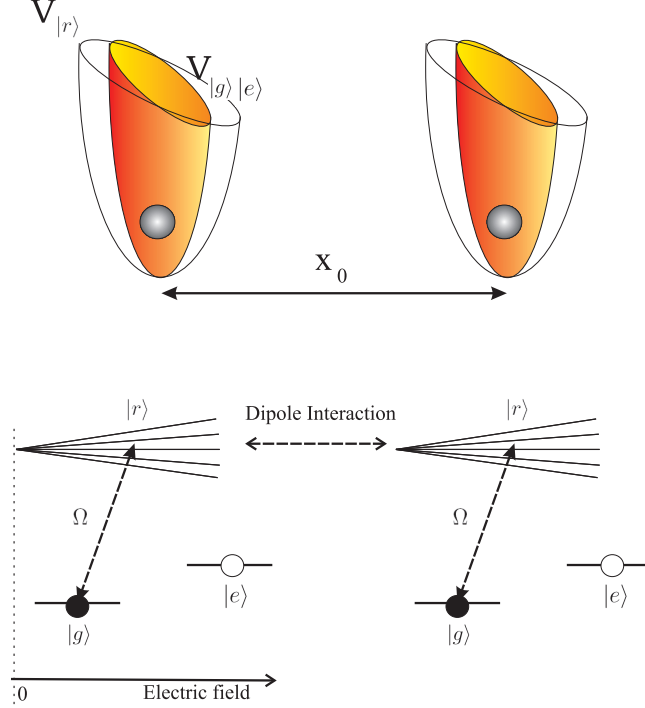


Fig. 2. Level scheme for the quantum phase gate. The internal state  $|g\rangle$  is coupled by the Rabi frequency  $\Omega$  to the Rydberg state  $|r\rangle$ . Since the state  $|e\rangle$  is unaffected by the laser, the dipole interaction arises only if both atoms are initially in the  $|g\rangle$  state. The harmonic trapping potential  $V_{|r\rangle}$  felt by the atoms in the Rydberg level  $|r\rangle$  is different from the potential  $V_{|g\rangle,|e\rangle}$  of the hyperfine levels  $|e\rangle$  and  $|g\rangle$ .

### 3.1 The dipole-dipole interaction

We consider two atoms in two different one-dimensional harmonic wells with the same frequency  $\omega$ , separated by a distance  $x_0$ . This system can be thought of as an approximate description of two atoms sitting in different sites of a optical lattice or in distinct trap minima on an atom chip, where the dynamics transverse to the direction joining the atoms are completely frozen. We will come back on such an approximation in Subsec. 3.3. Each atom corresponds to one qubit, where two internal hyperfine atomic levels, which we call  $|g\rangle$  and  $|e\rangle$ , represent the logical states.

Assuming an underlying static electric field, the gate is performed by driving state-dependent transitions to Rydberg levels (see Fig. 2), switching on and off a dipole atom-atom interaction which allows to manipulate the global phase of the system, as described in Ref. [7]. Initially, each atom can be either in  $|g\rangle$  or  $|e\rangle$ . The internal state  $|g\rangle$  is coupled by a laser to a Rydberg state  $|r\rangle$ , where the transition  $|g\rangle \rightarrow |r\rangle$  is assumed to be obtained via a Doppler-free two-photon absorption, which suppresses any photon kick contribution and gives rise to an effective Rabi frequency  $\Omega$  (see Fig. 2). The state  $|e\rangle$  is instead

fully decoupled from the Rydberg manifold. In this way, we switch on a dipole-dipole interaction only when both atoms are initially in the internal state  $|g\rangle$ . This interaction is kept on for a very short time, after which the atoms are brought back to the  $|g\rangle$  states. While in the  $|rr\rangle$  state, the atoms acquire a dynamical phase as well as a momentum shift (kick). Thus, repeating this procedure according to the scheme described in Sec. II, such a process realizes the phase gate (1), provided we undo the  $\pi$ -phase due to the Rabi flopping for the states  $|ge\rangle$  and  $|eg\rangle$ .

The Hamiltonian of the system without the laser coupling between the states  $|g\rangle$  and  $|r\rangle$  reads

$$\begin{aligned}
H = & \sum_{i=1,2} \left[ \frac{p_i^2}{2m} + \frac{1}{2}m\omega^2(x_i - x_{0i})^2 \right] (|g\rangle_i\langle g| + |e\rangle_i\langle e|) \\
& + \sum_{i=1,2} \left[ \frac{p_i^2}{2m} + \frac{1}{2}m\omega'^2(x_i - x_{0i})^2 \right] |r\rangle_i\langle r| \\
& + V_{\text{dip}}(x_1 - x_2)|r\rangle_1\langle r| \otimes |r\rangle_2\langle r|
\end{aligned} \tag{3}$$

where we consider that the (harmonic) trapping potential is the same for the two hyperfine levels (frequency  $\omega$ ) and different for the Rydberg state (frequency  $\omega'$ ). The general 3D expression for the dipole-dipole interaction is

$$V_{\text{dip}}(\mathbf{r}) = \frac{1}{4\pi\epsilon_0} \left[ \frac{\boldsymbol{\mu}_1 \cdot \boldsymbol{\mu}_2}{|\mathbf{r}|^3} - 3 \frac{(\boldsymbol{\mu}_1 \cdot \mathbf{r})(\boldsymbol{\mu}_2 \cdot \mathbf{r})}{|\mathbf{r}|^5} \right], \tag{4}$$

where  $\boldsymbol{\mu}_1, \boldsymbol{\mu}_2$  are the dipole moments of the two atoms, which depend on the Rydberg level and the external electric field, and the 3D relative distance  $\mathbf{r}$  reduces in our case to the 1D relative motion coordinate  $x = x_2 - x_1$ . In the Hamiltonian (3)  $m$  is the mass of the atoms and we take  $x_{02} - x_{01} = x_0$ , where  $x_0$  is the distance separating the two harmonic wells (see Fig. 2).

The possibility of exploiting this interaction to gain a non-trivial phase shift and effect a quantum gate has been suggested in Model A of Ref. [7]. In this scenario, during the interaction time  $\Delta t$ , the system acquires a dynamic phase  $u\Delta t$ , where  $u$  is the energy shift created by the dipole potential. However, in order to reproduce the truth table (1), one also has to ensure the restoring of the initial motional states, which are strongly affected by the non-negligible mechanical effects caused by the dipole interaction – and this is not straightforward in this scheme. To overcome this, in Ref. [7] a Model B has been introduced, where the strong dipole-dipole interaction is instead used to induce a dipole-blockade mechanism that still ensures state-dependent dynamics while actually avoiding mechanical back-action on the atomic motion.

An alternative solution can be achieved by controlling such strong mechanical

effects to gain an additional geometrical phase, while at the same time bringing the system back to the initial motional configuration, similarly to the method proposed in Ref. [11].

In the following we will consider only two possible configurations for  $V_{\text{dip}}(x)$ : the repulsive case  $V_+(x) = \mu_1\mu_2/4\pi\epsilon_0x^3$ , corresponding to dipoles aligned in the direction orthogonal to the  $x$ -axis, and the attractive case  $V_-(x) = -2\mu_1\mu_2/4\pi\epsilon_0x^3 = -2V_+(x)$ , corresponding to dipoles parallel to the  $x$ -axis. This in principle could be achieved by rapidly changing the electric field orientation between subsequent laser pulses – although from a practical point of view it may be problematic to realize this on the time scales required here. A viable alternative would be to keep the external field fixed and excite the system to Rydberg states having differently oriented dipole moments, something that could be performed without requiring individual laser addressing of the atoms.

The expression of the dipole moment for Rydberg states is given by  $\mu_{1,2} = (3/2)n_{1,2}q_{1,2}ea_0$  [14], where  $e$  is the electron charge,  $a_0$  is the Bohr radius, and  $n, q$  are quantum numbers which label the different states. The quantum number  $q$  obeys the relation  $q = n - 1 - |m|, n - 3 - |m|, \dots, -(n - 1 - |m|)$ , where  $m$  is the magnetic quantum number. Typical values considered here (for  $^{87}\text{Rb}$ ) are  $n_{1,2} = q_{1,2} + 1 = 50$ .

We prefer to work with dimensionless quantities by using the oscillator units of the harmonic potential with frequency  $\omega$ , felt by the atoms for most of the time. The dipole potential in particular can be rewritten as  $V_+/\hbar\omega = \alpha_+^2/(x/a_{\text{ho}})^3$ , where  $\alpha_+^2 = (9/4)n_1q_1n_2q_2(\mu/m_e)/(a_{\text{ho}}/a_0)$ ,  $\mu = m/2$  is the reduced mass,  $m_e$  is the electron mass, and  $a_{\text{ho}} = \sqrt{\hbar/\mu\omega}$  is the harmonic oscillator length and then we put  $\hbar = \mu = a_{\text{ho}} = 1$ .

Note that in order to realize an ideal transition to the Rydberg state one needs the condition  $\Omega \gg |V_{\pm}(x_0)|$ , i.e.,  $\Omega \gg 2\alpha_+^2/x_0^3$ , which is easily satisfied in all the cases of practical interest. Realistic values for the parameters are discussed in Subsec. 3.3.

We describe the action of the dipole potential arising when both atoms are in a Rydberg state by using an impulse approximation. We indeed assume that the dipole interaction is very strong compared to the harmonic trapping and that its duration is very short, so that the system undergoes a small displacement during this time and the corresponding harmonic potential contribution to the phase is negligible. Furthermore we separate the centre of mass and relative motion, where only the latter is affected by the dipole-dipole interaction. Due to the very short time spent by the atoms in the Rydberg state, we then consider the centre of mass motion to be completely unperturbed by the gate and will only examine the relative motion. For a short time interval  $\Delta t$  the

relative motion time evolution operator can hence be approximated by

$$U_{\Delta t} \simeq e^{-iV_{\text{dip}}(x)\Delta t} , \quad (5)$$

where, in force of the impulse approximation, we dropped both the kinetic term and the harmonic oscillator potential. In addition, we expand the dipole potential around the centre  $x_0$  of the harmonic trap

$$V_{\text{dip}}(x) \simeq V_{\text{dip}}(x_0) + V'_{\text{dip}}(x_0)(x - x_0) , \quad (6)$$

where the prime denotes the first spatial derivative. The largest possible value of  $|x - x_0|$  is fixed by the extension of the relative motion wavefunction  $\psi$ . This can be quantified by the average position  $\langle x \rangle = \int x |\psi|^2 dx$  and the mean square length  $\langle \Delta x \rangle = \sqrt{\langle x^2 \rangle - \langle x \rangle^2}$ , so that the validity of the linear approximation (6) requires<sup>3</sup>  $|x - x_0| \lesssim |\langle x \rangle - x_0| + \langle \Delta x \rangle \ll x_0$ . A full description of the consequences of the above conditions in terms of experimental parameters is given in Subsec. 3.3.

With the previous approximations the time evolution operator acquires the elementary form

$$U_{\Delta t} \simeq e^{-iu\Delta t + i\Delta p(x-x_0)} , \quad (7)$$

where  $u = V_{\text{dip}}(x_0)$  is the zero-energy shift and the momentum transfer ('kick')  $\Delta p$  is simply given by the classical expression  $\Delta p = -V'(x_0)\Delta t$ .

### 3.2 The dynamical phase

The 'ideal' picture described in Section 2 can now be joined with the actual form of the kick dynamics. The phase space depicted in Fig. 1 will clearly correspond to the relative motion harmonic oscillator with frequency  $\omega$  (which scales to 1 in dimensionless units), whereas the kicks will be provided by the dipole potential. As previously discussed, in first approximation one has  $p_1 = |V'_+(x_0)\Delta t_1|$  and  $p_2 = |V'_-(x_0)\Delta t_2|$ , i.e., the momentum transfers  $p_{1,2}$  require a finite (although very short, as far as  $V_{\text{dip}}$  is large) time  $\Delta t_{1,2}$ . In addition, since  $p_2 = 2p_1 \cos \theta$  and<sup>4</sup>  $V'_-(x_0) = -2V'_+(x_0)$ , one has  $\Delta t_2 = \Delta t_1 \cos \theta$ . The total phase  $\phi$  gained by the system is the sum of the dynamical phase

<sup>3</sup> One could improve this approximation by linearizing  $V_{\text{dip}}(x)$  around  $\langle x \rangle$  instead of  $x_0$ . This, however, would make the calculation dependent on the initial motional state. A proper discussion of the corresponding procedure could be done within the optimal control technique.

<sup>4</sup> Here we assume that all the kicks are obtained by coupling the atoms to the same Rydberg state, choosing the simplest experimental situation where only one laser frequency is required. In principle, nothing prevents from using more complicated schemes which add further degrees of freedom to the protocol.

$\phi_{\text{dyn}} = -[V_+(x_0)\Delta t_1 + V_-(x_0)\Delta t_2 + V_+(x_0)\Delta t_1] = -2V_+(x_0)\Delta t_1(1 - \cos \theta)$  and the geometrical phase  $\phi_{\text{geom}}$ . Hence

$$\phi = -2\frac{\alpha_+^2}{x_0^3}\Delta t_1(1 - \cos \theta) - \frac{9}{2}\frac{\alpha_+^4}{x_0^8}\Delta t_1^2 \sin(2\theta) , \quad (8)$$

which can be solved to give

$$\alpha_+^2 \Delta t_1 = \frac{2}{9} \frac{x_0^5}{\sin(2\theta)} \left[ \cos \theta - 1 + \sqrt{(\cos \theta - 1)^2 + \frac{9}{2} \frac{\sin(2\theta)}{x_0^2} |\phi|} \right] . \quad (9)$$

This allows to choose the proper combination of Rydberg quantum numbers and interaction time in order to achieve the desired phase. The full gate time required by the operation will be  $\tau = \Delta t_1(2 + \cos \theta) + 2\theta \sim 2\theta$ . It is also interesting to consider the fast quantum gate limit  $\theta \rightarrow 0$  where one easily finds  $\alpha_+^2 \Delta t_1 \sim (x_0^4/3)\sqrt{|\phi|/\theta}$ . This implies  $\phi_{\text{dyn}} \sim -(x_0/3)\theta^{3/2}\sqrt{|\phi|}$  and  $\phi_{\text{geom}} \sim \phi$ , which means that in this limit the global phase  $\phi$  is completely given by the geometrical contribution.

Let us stress again that the phase  $\phi$  will arise only if the atoms are initially in the  $|gg\rangle$  internal state, since otherwise the dipole potential is never switched on.

### 3.3 Validity of the employed approximations

Our impulse approximation (5) requires that, during the interaction time  $\Delta t$ , the action of the relative motion oscillator Hamiltonian  $H_0 = p^2/2 + (x - x_0)^2/2$  (we keep on using harmonic oscillator units) be negligible<sup>5</sup>. The contributions of the different terms in the Hamiltonian can be quantified at a given time by taking their expectation values on the corresponding state  $|\psi(t)\rangle$ . We therefore require

$$\langle H_0 \rangle \ll |\langle V_{\text{dip}} \rangle| \quad (10)$$

during the whole kick time  $\Delta t$ . However, from the point of view of the gate dynamics, it is also necessary to have

$$\langle H_0 \rangle \Delta t \ll |\phi| , \quad (11)$$

since otherwise we should include such a contribution in the calculation of the dynamical phase  $\phi_{\text{dyn}}$ .

<sup>5</sup> In this analysis we assume for simplicity that  $\omega$  and  $\omega'$  are of the same order [7].

Besides conditions (10) and (11), we also have to consider the validity requirements of the linear approximation (6), i.e., the condition

$$|\langle x \rangle - x_0| + \langle \Delta x \rangle \ll x_0 , \quad (12)$$

necessary for the linearization of the dipole potential. Clearly, the explicit form of all the previous conditions depends on the states reached by the system during the dynamics of the kick scheme.

For example, if the system stays very close to the oscillator ground state during the whole gate time, one can estimate the above expectation values by using  $|\psi(t)\rangle = |0\rangle$ . In this case  $\langle H_0 \rangle = 1/2$ ,  $\langle x \rangle = x_0$  and  $\langle \Delta x \rangle = 1/\sqrt{2}$ . Linearization then requires  $x_0 \gg 1/\sqrt{2}$ , while, by assuming the validity of the latter condition, Eq. (10) reduces to  $1/2 \ll V_+(x_0)$ , which can be made explicit by evaluating  $V_+(x_0) = \alpha_+^2/x_0^3$  with Eq. (9). Eq. (11) is simply  $\Delta t \ll 2|\phi|$ .

Since we want our protocol to be independent of the initial motional state, it is interesting to find the conditions under which our approximations are applicable to a generic state *not too far* from the ground state. We therefore consider the case  $|\psi(t)\rangle = |\alpha(t)\rangle$ , where  $|\alpha(t)\rangle$  is a coherent state subject to the constraint  $|\alpha(t)| \leq R$ ,  $R > 0$ . Then, if the initial state of the system is the coherent state  $|\alpha(0)\rangle$ , the boundary  $R$  can be estimated within the ideal kick scheme, where  $|\alpha(t)| \leq |\alpha(0)| + \tilde{p}_1$ . Concerning the expectation values we have  $\langle H_0 \rangle = |\alpha|^2 + 1/2 \leq R^2 + 1/2$ ,  $|\langle x - x_0 \rangle| = \sqrt{2} |\operatorname{Re} \alpha| \leq \sqrt{2} R$ , and still  $\langle \Delta x \rangle = 1/\sqrt{2}$ . If  $x_0 \gg \sqrt{2} R + 1/\sqrt{2}$  then the use of the linear approximation is legitimate and Eq. (10) becomes  $R^2 + 1/2 \ll V_+(x_0)$ , while Eq. (11) is  $(R^2 + 1/2)\Delta t \ll 2|\phi|$ .

We explicitly evaluate these conditions for the most interesting case  $\alpha(0) = 0$ , where initially the system is in the oscillator ground state and hence  $R = \tilde{p}_1 = (3/\sqrt{2})V_+(x_0)\Delta t_1/x_0$ . Qualitatively, fast gate performances require small values of  $\theta$ , while the linear approximation (6) needs large values of  $x_0$ . However large distances disfavour the impulse approximation (5), which is valid for strong dipole interactions. High Rydberg quantum numbers are then necessary to enhance the dipole moments. In order to study the interplay among the different parameters it is useful to consider Eq. (9) in the limits  $\theta \rightarrow 0$  and  $x_0 \rightarrow \infty$ . Then, it turns out that in all the cases of practical interest condition (10) is already implied by Eqs. (11) and (12), so that one is left with only two conditions. In addition, the most stringent form of these requirements takes place in the  $\theta \rightarrow 0$  limit, where  $V_+(x_0)\Delta t_1 \sim (x_0/3)\sqrt{|\phi|/\theta}$ . In conclusion, the linearization condition (12) and Eq. (11) respectively reduce to

$$x_0 \gg \sqrt{|\phi|/\theta} , \quad (13)$$

$$\Delta t_1 \ll 2\theta , \quad (14)$$

valid in the fast-gate limit  $\theta \rightarrow 0$ .

The conditions (13-14) are actually rather demanding in terms of experimental parameters, even though certainly achievable. Assuming Eqs. (13) and (14) to be well satisfied by a factor of ten difference between the two terms of each inequality, so that  $x_0 = 10\sqrt{|\phi|/\theta}$  and  $\Delta t_1 = \theta/5$ , and recalling the  $\theta \rightarrow 0$  result  $\alpha_+^2 \sim (x_0^4/3\Delta t_1)\sqrt{|\phi|/\theta}$ , one gets  $\alpha_+^2 \sim (10^5/6\theta)(|\phi|/\theta)^{5/2}$ . Unfortunately,  $\alpha_+^2$  cannot be arbitrarily large. For example, for the case of  $^{87}\text{Rb}$  atoms, where  $\mu = 87/2$  amu, with a harmonic frequency  $\omega = 2\pi \times 100$  KHz, so that  $(\mu/m_e)/(a_{\text{ho}}/a_0) = 86.8$ , by choosing the Rydberg quantum numbers  $n_{1,2} = q_{1,2} + 1 = 50$  one has  $\alpha_+^2 = 1.2 \times 10^9$ . Then, for  $|\phi| = \pi$  (equivalent to the C-NOT gate), the shortest gate-time obtainable within this rough upper bound for  $\alpha_+^2$  corresponds to  $\theta = [(10\sqrt{|\phi|})^5/6\alpha_+^2]^{2/7} = 0.09$ , i.e.,  $\tau \sim 0.03T_{\text{ho}}$ , where  $T_{\text{ho}} = 2\pi$  is the harmonic oscillator period. Notice also that, while the condition corresponding to Eq. (14),  $\Delta t_1 = \theta/5$ , can be easily satisfied experimentally, Eq. (13) for such a small value of  $\theta$  imposes a very large separation between the harmonic wells (in harmonic oscillator units), namely  $x_0 = 10\sqrt{|\phi|/\theta} = 58$ , significantly larger than the value corresponding to the typical distance between neighbouring sites in currently employed optical lattices (for example, for a laser wavelength of 800 nm, the above parameters yield  $x_0 = 8.3$ ). However, this requirement can be clearly relaxed by increasing the gate time (see the next section). Besides, there is the possibility of increasing  $x_0$  independently of the lattice spacing, e.g., by using superlattices or the methods discussed in Ref. [15].

In the final part of this section, we briefly discuss the validity of the one-dimensional approximation (see also [7]). We assume a harmonic trapping also in the radial direction, with a frequency  $\omega_{\perp}$  and restore the dimensional units. The radial degrees of freedom could then be neglected if the level spacing  $\hbar\omega_{\perp}$  were much larger than all the other energy scales which come into play. Clearly, this is difficult to accomplish as far as one also needs large values of the frequency  $\omega$  along the  $x$  direction, necessary to increase the ratio  $x_0/a_{\text{ho}} \propto \sqrt{\omega}$ . However, provided each atom is sitting in the ground state of the corresponding harmonic well, the dimensionality does not play any role. Indeed, assuming the exact dipole polarization, the momentum transfer takes place only in the  $x$  direction and the gate dynamics is decoupled from the radial degrees of freedom, irrespectively of the value of  $\omega_{\perp}$ . In the case where the initial motional state significantly differs from the ground state, one instead has to compare  $\hbar\omega_{\perp}$  with  $\hbar\omega$  and with the component of the dipole potential affecting the radial motion, which is however smaller and smaller as the inter-well distance increases. Consequently, the validity condition of the linear approximation also favours the quenching of 3D effects, even though a quantitative analysis of this approximation would require a full description of the 3D dynamics, which is beyond the scope of this paper.

## 4 Fidelity analysis

We are now interested in considering possible error sources. The effects we take into account in the following are (i) contributions not included in the impulse and kick approximations, which are important when the validity conditions discussed in the previous section are not well satisfied, and (ii) anharmonic terms in the trapping potential. Notice that, since as far as our approximations are valid the model is independent of the initial motional state, finite ‘temperature’ (in a sense specified later) effects are actually included in the first point.

Note that in addition, as discussed in [7], minor error sources that are completely neglected here are the spontaneous emission and the black body radiation for the Rydberg state.

In our scheme atoms in different wells have a negligible overlap and can be considered distinguishable. In this case the gate fidelity can be defined as [16]

$$F = \min_{\chi} \{ \text{Tr}_{\text{ext}} [\langle \tilde{\chi} | \mathcal{U}_{\tau} (|\chi\rangle\langle\chi| \otimes \rho_0) \mathcal{U}_{\tau}^{\dagger} | \tilde{\chi} \rangle] \} , \quad (15)$$

where  $\mathcal{U}_{\tau}$  is the unitary operator governing the evolution of the full system during a single gate operation,  $|\chi\rangle = \sum_{\alpha\beta} c_{\alpha\beta} |\alpha\beta\rangle$  is an arbitrary internal state of the two atoms with the normalization  $\sum_{\alpha\beta} |c_{\alpha\beta}|^2 = 1$ ,  $|\tilde{\chi}\rangle$  is the state given by the application of the ideal gate (1) to  $|\chi\rangle$ , and  $\rho_0$  is the initial density operator relative to the external degrees of freedom, over which the trace is taken. In our case, the external states are simply given by the motional states. Furthermore, since the centre of mass motion is unaffected by the gate, we can restrict the analysis to the relative motion<sup>6</sup>.

### 4.1 Fidelity for pure motional states

Let us consider the particular case  $\rho_0 = |k\rangle\langle k|$ , where  $|k\rangle$  are the eigenstates of the relative motion harmonic oscillator. This corresponds to assuming zero entropy, the system being in a pure state.

We can write the action of  $\mathcal{U}_{\tau}$  as

---

<sup>6</sup> This is not generally true, e.g., if the atoms were in the internal state  $|er\rangle$  for a time comparable with the oscillator time scales.

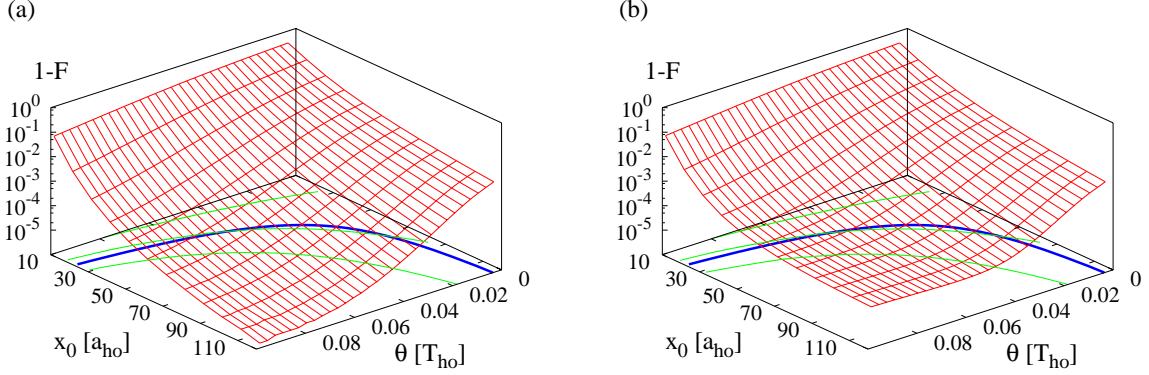


Fig. 3. Upper panel (a): fidelity  $F = (1 + \text{Re}\langle\psi_{\text{id}}|\psi_{\text{num}}\rangle)/2$  as a function of the time  $\theta$  and the distance  $x_0$  (harmonic oscillator units), for  $|\phi| = \pi$  and  $\Delta t_1 = 10^{-4} \times 2\pi$ . The state  $|\psi_{\text{num}}\rangle$  is obtained by calculating numerically the full gate-dynamics (in the absence of anharmonic perturbations) for the state  $|gg\rangle \otimes |0\rangle$ , while the ideal state is simply  $|\psi_{\text{id}}\rangle = e^{i\phi}|0\rangle$ . The contour lines drawn in the lower plane correspond to the fidelity values 0.9, 0.99, 0.999, while the thick line plots the relation  $x_0 = 10\sqrt{\pi/\theta}$ . Lower panel (b): same as (a) but in the presence of an anharmonic quartic term with  $\lambda = 10^{-2}$ .

$$\begin{aligned} \mathcal{U}_\tau(|\chi\rangle \otimes |k\rangle) &= \sum'_{\alpha\beta} c_{\alpha\beta} |\alpha\beta\rangle \otimes |k\rangle e^{-i(k+1/2)\tau} + \\ &+ c_{gg} |gg\rangle \otimes \sum_{k'} \alpha_{kk'} |k'\rangle e^{-i(k'+1/2)\tau}, \end{aligned} \quad (16)$$

where the primed summation does not contain the term  $\alpha\beta = gg$ , and  $\sum_{k'} |\alpha_{kk'}|^2 = 1$ . The explicit calculation then gives

$$\begin{aligned} F_k &= \min_{|c_{gg}|} \{1 + 2(1 - |c_{gg}|^2) |c_{gg}|^2 [\text{Re}(e^{i\phi} \alpha_{kk}^*) - 1]\} = \\ &= \frac{1 + |\alpha_{kk}| \cos(\phi - \phi_{kk})}{2}, \end{aligned} \quad (17)$$

where  $\phi_{kk} = \arg \alpha_{kk}$  and  $e^{i\phi} \alpha_{kk}^* = \langle\psi_{\text{num}}(k)|\psi_{\text{id}}(k)\rangle$  is the overlap between  $|\psi_{\text{id}}(k)\rangle = e^{i\phi}|k\rangle$  and the final motional state obtained by applying the full gate dynamics to the state  $|gg\rangle \otimes |k\rangle$ .

We compute the zero-entropy fidelity in the good initialization case  $k = 0$ . In the ideal case where the impulse approximation is valid one has  $\alpha_{00} = e^{i\phi_{00}} = e^{i\phi}$  and  $\alpha_{0k} = 0$  for  $k \geq 1$ .

In Fig. 3(a) we show the gate fidelity  $F$  when the protocol is applied to the motional ground state ( $k = 0$ ), as a function of the two most important parameters  $\theta$ ,  $x_0$ . This allows a direct comparison with the conditions discussed in Subsec. 3.3. The data are obtained by solving numerically the time dependent Schrödinger equation corresponding to the full kick dynamics applied

to the oscillator ground state, for the case of purely harmonic trapping. The behaviour corresponding to Eq. (13) is also plotted, showing a qualitative agreement with the curves at constant fidelity. Indeed, for the considered parameters, Eq. (14) is always very well satisfied and the terms not included in the linear approximation are the main reason of discrepancy with respect to the ideal scheme.

In Fig. 3(b) we repeat the same analysis by adding to  $H_0$  an anharmonic term  $-\lambda(x - x_0)^4/2$ , corresponding to the first correction one would have for the square sinus potential of an optical lattice<sup>7</sup>. Only a very slight worsening of the fidelity is observed for the realistic value  $\lambda = 10^{-2}$ , showing that in practice the validity of the linear approximation is the crucial condition.

#### 4.2 Finite temperature and entropy effects

In view of a realistic quantum computing scenario it is important to investigate the dependence of the gate performances on temperature. Indeed, in the course of the computational process the system is expected to undergo a certain heating – for example due to moving the atomic qubits around by shifting the optical lattice – which could in principle be limited by a periodic re-cooling of the qubits [17].

On the other side, atoms in optical lattices can be considered practically isolated from the environment, so that in the experimental setup considered here atoms do not easily thermalize. An alternative interesting quantity to study is hence given by entropy, whose value can be extracted from the density matrix of the system.

Let us first discuss the fidelity of the gate in the case where the density matrix of the relative motion is given by the canonical thermal distribution

$$\rho_{\text{rel}}(T) = 2 \sinh \frac{E_0}{k_B T} \sum_k e^{-E_k/k_B T} |k\rangle \langle k|, \quad (18)$$

where  $T$  is the temperature,  $k_B$  is the Boltzmann constant, and  $E_k$  are the oscillator energies. The density operator satisfies the normalization  $\text{Tr}[\rho_{\text{rel}}(T)] = 1$ .

---

<sup>7</sup> Actually, the square sinus potential enters the single atom Hamiltonians. In this case it is not even possible to exactly separate the centre of mass and relative motion Hamiltonians. Such decoupling is indeed a peculiar property of the harmonic potential. However, the quartic correction can be used as a crude test of anharmonic effects.

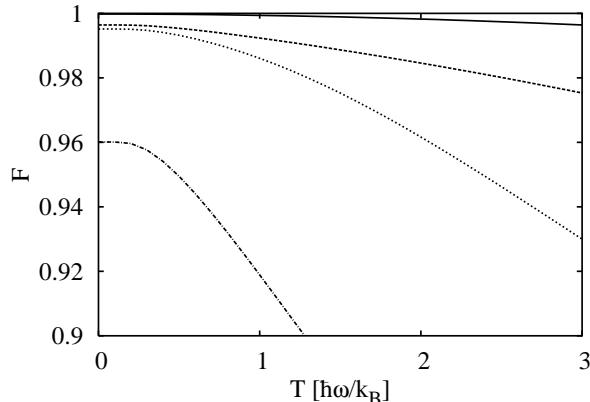


Fig. 4. Temperature dependence of the fidelity ( $|\phi| = \pi$ ,  $\Delta t_1 = 10^{-4}T_{\text{ho}}$ ,  $\lambda = 0$ ). Curves from top to bottom correspond to  $\theta = 0.05T_{\text{ho}}$ ,  $x_0 = 20$  (solid line),  $\theta = 0.05T_{\text{ho}}$ ,  $x_0 = 40$  (dashed line),  $\theta = 0.1T_{\text{ho}}$ ,  $x_0 = 20$  (dotted line),  $\theta = 0.1T_{\text{ho}}$ ,  $x_0 = 40$  (dot-dashed line).

By substituting  $\rho_0 = \rho_{\text{rel}}(T)$  into Eq. (15), the fidelity of the finite temperature motional state is found to be

$$F = 2 \sinh \frac{E_0}{k_B T} \sum_k e^{-E_k/k_B T} F_k, \quad (19)$$

where  $F_k$  is given in Eq. (17). The resulting behaviour for reasonable values of the (purely harmonic,  $\lambda = 0$ ) trap parameters is reported in Fig. 4. Notice that current experimental techniques allow to cool the system much below the highest temperature considered in the figure (which is three times the temperature defined by the oscillator energy). In the numerical calculation, for each considered temperature the density matrix is constructed by including in Eq. (18) all the eigenstates up to at least  $E_k = 5k_B T$ . It is worth mentioning that the presence of anharmonicities in the trapping potential can worsen the large temperature behaviour of the curves shown in Fig. 4. Indeed, higher oscillator states, having a larger spatial extension, are more sensitive to deviations from the quadratic confinement. However, for a quartic term with  $\lambda = 10^{-2}$  (see previous subsection) and the parameters of Fig. 4 this becomes important only for  $k_B T \gtrsim 3$  (corresponding to the mean occupation number  $\bar{k} \sim 2.5$ ).

As anticipated above, it is also useful to look at the entropy increase caused by the gate evolution. In fact, even if the very first initialization was perfectly done, i.e.,  $\rho_0 = |0\rangle\langle 0|$ , after a certain number of operations one expects the system to be in a superposition of excited motional states. As shown by Eq. (16), already after a single 2-qubit gate the system is left in a non-trivial, entangled state of the internal and external degrees of freedom, which will spoil to some extent a successive application of the phase gate. Clearly, for the gate to make sense this must be a small effect, which is guaranteed by fidelity values close

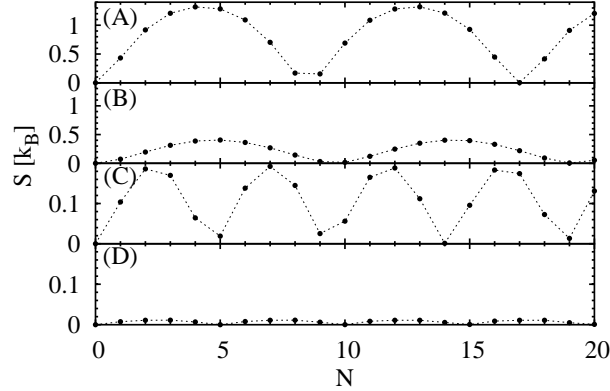


Fig. 5. Entropy  $S$  (in units of  $k_B$ ) as a function of the number of cycles  $N$  for  $|\phi\rangle = \pi$  and  $\Delta t_1 = 10^{-4}T_{\text{ho}}$ . The considered trapping potential is the purely harmonic ( $\lambda = 0$ ) and the remaining parameters are (A)  $\theta = 0.05T_{\text{ho}}$ ,  $x_0 = 20$ , (B)  $\theta = 0.05T_{\text{ho}}$ ,  $x_0 = 40$ , (C)  $\theta = 0.1T_{\text{ho}}$ ,  $x_0 = 20$ , (D)  $\theta = 0.1T_{\text{ho}}$ ,  $x_0 = 40$ .

to 1. Qualitatively, it is also interesting to see which is the fidelity for the finite entropy states arising from repeated executions of the gate operation. Indeed, although in practice computation would not involve always the same two qubits, this gives an idea of the propagation of the gate error.

Concretely, if we start with the system in the product state  $|\Psi\rangle = |\chi\rangle \otimes |0\rangle$ , with the same notation as in the previous subsection, after  $N$  gate operations  $|\Psi\rangle$  is transformed into the  $N$ -step state  $|\Psi(N\tau)\rangle = c_{gg}|gg\rangle \otimes \sum_k \alpha_{0k}(N\tau)|k\rangle e^{-i(k+1/2)N\tau} + (c_{ge}|ge\rangle + c_{eg}|eg\rangle + c_{ee}|ee\rangle) \otimes |0\rangle e^{-iN\tau/2}$ . For simplicity, we consider the case  $c_{gg} = 1$  and construct a relative motion density matrix with the  $N$ -step coefficients  $\alpha_k(N\tau)$

$$\rho_{\text{rel}}(N) = \sum_k |\alpha_{0k}(N\tau)|^2 |k\rangle\langle k|. \quad (20)$$

The entropy is  $S = -k_B \text{Tr}[\rho_{\text{rel}}(N) \ln \rho_{\text{rel}}(N)]$ , where the trace can be calculated summing over all the eigenvalues, already explicit in the diagonal form of Eq. (20).

The entropy behaviour as a function of the number of gate cycles is plotted for reasonable parameters in Fig. 5. In the numerical calculation the entropy is extracted by projecting the time-evolved state onto the harmonic oscillator eigenstates  $|n\rangle$ . All the eigenstates up to  $n = 25$  are included, much more than required for the considered parameters, ensuring that the normalization is always preserved. The maximum (numerical) entropy is  $S/k_B = \ln n \sim 3.2$ . Note the periodic behaviour of the entropy: its value does not increase arbitrarily. Indeed, after a given number of cycles one has a revival of the initial state (i.e., only the relative motion ground state is occupied). This is true only for reasonable parameters: for parameters which yield a bad gate fidelity one does not have this revival and the entropy increases monotonically.

As an estimate of the fidelity due to a non-zero entropy motional state we use

	$\theta = 0.05 T_{\text{ho}}$	$\theta = 0.1 T_{\text{ho}}$
$x_0 = 20$	$F_0=0.9601$	$F_0=0.9952$
	$F(N = 4)=0.8889$	$F(N = 2)=0.9946$
	$S(N = 4)=1.32$	$S(N = 2)=0.19$
$x_0 = 40$	$F_0=0.9964$	$F_0=0.9998$
	$F(N = 4)=0.9956$	$F(N = 2)=0.9998$
	$S(N = 4)=0.39$	$S(N = 4)=0.01$

Table 1

Fidelity of a single gate execution at different entropy values for the same parameters as in Fig. 5.  $F_0$  is the fidelity calculated for the matrix  $|\chi\rangle\langle\chi| \otimes |0\rangle\langle 0|$  (zero entropy), while  $F(N)$  for the matrix  $|\chi\rangle\langle\chi| \otimes \rho_{\text{rel}}(N)$ . The entropy  $S(N)$  is the same shown in Fig. 5.

Eq. (15) with  $\rho_0 = |\chi\rangle\langle\chi| \otimes \rho_{\text{rel}}(N)$ . The calculation now gives

$$F = \sum_k |\alpha_{0k}(N\tau)|^2 F_k, \quad (21)$$

and the corresponding results for some relevant values of  $N$  are reported in Table 1, showing that the fidelity is not affected very much by the considered process. Indeed, for the used parameters the coefficients  $|\alpha_{0k}(N\tau)|^2$  entering Eq. (20) decay very rapidly by increasing  $k$ . In other terms, although not directly comparable to the canonical distribution (18), the population of the first few states shows a behaviour corresponding to  $k_B T \ll 1$  (in harmonic oscillator units). As a consequence, we also notice that the small anharmonicity ( $\lambda = 10^{-2}$ ) previously considered does not alter significantly the results presented in Table 1 for the purely harmonic case.

## 5 Conclusions and outlook

In this paper we aimed at applying the method of coherent control of two-body dynamics, already proposed in [11] as a means for obtaining fast, high-fidelity quantum gates with ions, to the case of Rydberg-excited atoms. We found that the method works well in a realistic situation with a simple three-pulse sequence that allows for obtaining a two-qubit control-phase gate with a fidelity bigger than 99.9% in a fraction of the trap period for presently achievable experimental parameters. While the ideal scheme at the basis of the gate is completely independent of the initial motional state of the atoms, the approximations employed to treat the dipole-dipole interaction introduce deviations which worsen the gate performance for motional states different from the ground state. We then analyze the effect of errors in the preparation

of the motional state in terms of temperature and entropy. For parameters reasonably close to the ones optimized for high fidelity, the temperature of the initial state is found to significantly affect the gate quality only for relatively large values, comparable with the oscillator energy of the trapping potential. In addition, the entropy of the evolved state obtained from repeated applications of the gate to the same two qubits does not increase indefinitely with the number of operations, but it rather oscillates in a quite regular fashion, exhibiting full ground-state revivals after a few gate iterations. This is likely to depend on symmetries in the underlying evolution, evidenced by the trivial iteration of the gate on the same two qubits. Even though the latter analysis does not convey much information on a real quantum algorithm, which typically involves many gates between different qubits, it would be interesting to study the possibility that similar recurrences emerge over more complex gate sequences. In this case, indeed, optimization could be done not only at the level of a single quantum gate, but also on a broader time scale involving “blocks” of subsequent gates, in the sense of tailoring each gate’s parameters in order to minimize the system entropy after a given gate sequence. A deeper understanding of this aspect is still missing, as it goes beyond the scope of the present work, and shall be the subject of future investigations.

Let us finally comment on a possible alternative implementation of the phase-space displacements which allow to acquire the geometrical phase. Indeed, the momentum shifts obtained from the dipole kicks could in principle be substituted by spatial shifts, straightforwardly realizable by displacing the centre of the harmonic oscillator potential, provided that one manages to properly design the spin dependency of the trapping potential [18].

## Acknowledgements

This work was partially supported by the European Commission under Contracts No. IST-2001-38863 (ACQP), FP6-013501-OLAQUI, FP6-015714-SCALA, and by the National Science Foundation through a grant for the Institute for Theoretical Atomic, Molecular and Optical Physics at Harvard University and Smithsonian Astrophysical Observatory. Work at the University of Innsbruck is supported by the Austrian National Science Foundation and the EU projects.

## References

- [1] B. Shore, *The Theory of Coherent Atomic Excitation*, Vol. 2, Wiley-Interscience (1990).

- [2] J.I. Cirac and P. Zoller, Phys. Rev. Lett **74**, 4710 (1995); Q.A Turchette *et al.*, Phys. Rev. Lett **81**, 3631 (1998); T. Calarco, J.I. Cirac, and P. Zoller, Phys. Rev. A **63**, 062304 (2001).
- [3] Q.A Turchette *et al.*, Phys. Rev. Lett **75**, 4710 (1995); X. Maitre *et al.*, Phys. Rev. Lett **79**, 769 (1997); E. Hagley *et al.*, Phys. Rev. Lett **79**, 1 (1997); T. Pellizzari, S.A Gardiner, J.I. Cirac, and P. Zoller, Phys. Rev. Lett. **75**, 3788 (1995).
- [4] D.G. Cory, A.F. Fahmy, T.F. Havel, Proc. Natl. Acad. Sci. USA **94**, 1634 (1997); N.A. Gershenfeld, I.L. Chuang, Science **275**, 350 (1997).
- [5] See Fortschr. Phys. **48**, No. 9-11 (2000), special issue on quantum computing.
- [6] T. Calarco *et al.*, Phys. Rev. A **61**, 022304 (2000).
- [7] D. Jaksch *et al.*, Phys. Rev. Lett. **85**, 2208 (2000).
- [8] T. Calarco *et al.*, Phys. Rev. A **70**, 12306 (2004).
- [9] K. Singer *et al.*, Phys. Rev. Lett. **93**, 163001 (2004).
- [10] D. Tong *et al.*, Phys. Rev. Lett. **93**, 063001 (2004).
- [11] J.J. García-Ripoll, P. Zoller, and J.I. Cirac, Phys. Rev. Lett. **91** (2003) 157901.
- [12] J.J. García-Ripoll, P. Zoller, and J.I. Cirac, Phys. Rev. A **71** (2005) 062309 .
- [13] K. Singer, F. Schmidt-Kaler and T. Calarco, in preparation.
- [14] T.F. Gallagher, *Rydberg Atoms* (Cambridge University Press, New York, 1994).
- [15] L. Fallani, C. Fort, J. Lye, M. Inguscio, Opt. Express **13**, 4303 (2005).
- [16] B. Schumacher, Phys. Rev. A **54**, 2614 (1996).
- [17] A.J. Daley, P.O. Fedichev, and P. Zoller, Phys. Rev. A **69**, 022306 (2004).
- [18] O. Mandel, *et al.*, Phys. Rev. Lett. **91**, 010407 (2003).